



Influence of the intermediate layer on the hydrothermal stability of sol-gel derived hybrid silica membranes



Marcel ten Hove, Mieke W.J. Luiten-Olieman*, Cindy Huisjes, Arian Nijmeijer, Louis Winnubst

Inorganic Membranes, MESA+ Institute for Nanotechnology, University of Twente, P.O. Box 217, 7500 AE, Enschede, The Netherlands

ARTICLE INFO

Article history:

Received 12 January 2017

Received in revised form 17 March 2017

Accepted 19 March 2017

Available online 9 April 2017

Keywords:

Hydrothermal stability

Hybrid silica

Gas separation

Microporous membrane

Monoaluminumphosphate coating

ABSTRACT

The hydrothermal stability of microporous silica hybrid sol-gel derived membranes is often only tested for either the mesoporous intermediate membrane layer or the microporous separation layer. In this work an investigation is done on the interaction between the intermediate γ -alumina layer and the hybrid (BTESE-derived) silica separation layer during hydrothermal treatment. Although bare γ -alumina is degraded during a hydrothermal treatment, a coating of hydrophobic BTESE on γ -alumina retains its gas separation performance, albeit with a lower mechanical adhesion between the hybrid silica separation layer and the γ -alumina intermediate layer. Applying a monoaluminumphosphate (MAP) coating between the α -alumina support and the γ -alumina layer stabilizes the γ -alumina membrane. A BTESE coating on a MAP modified γ -alumina membrane did not show any signs of delamination after hydrothermal testing. Moreover, a significant increase in the H_2/N_2 (perm)selectivity, factor 3, was observed for these membranes.

© 2017 Elsevier Ltd. All rights reserved.

1. Introduction

The global energy consumption rapidly increases every year, resulting in a fast depletion of the energy resources. Several strategies are being developed to generate alternative, environmental friendly ways to produce and store energy. Using hydrogen as a fuel is one of them. Hydrogen can be produced via water electrolysis, steam methane reforming, coal gasification and water gas shift reaction [1]. One essential, critical step in the production of hydrogen is gas separation. Highly selective inorganic membranes are ideal candidates to perform this separation as they are able to operate at high temperatures, although the hydrothermal stability of these membranes is debated.

For the above mentioned applications sol-gel derived microporous ceramic membranes are frequently studied. These gas separation membranes are often made as a multi-graded system. A macroporous support provides the system its mechanical strength; a mesoporous layer provides a smooth surface and a pore size of several nanometers for the application of a defect free microporous separation layer with a pore size of less than 1 nm. The mesoporous layer is already a membrane by itself that can be used for

nanofiltration. A typical pore diameter for these mesoporous layer is around 5 nm. Commonly used materials as intermediate layer are γ -alumina [2,3], yttria stabilized zirconia [4] or silica-zirconia [5]. These mesoporous membranes provide a very well defined surface for the deposition of a sol-gel derived microporous top layer, which can have a thickness of only 100 nm or less and hence needs a very smooth surface as a basis.

The material that is widely used as mesoporous intermediate layer is γ -alumina due to the relatively easy way of fabrication and its high surface quality [6]. The hydrothermal stability of such γ -alumina layers is however rather poor. Gallaher et al. [7] showed for commercial γ -alumina membranes (Membralox[®], US Filter) that pore growth occurs, from 4.0 to 6.5 nm, after a hydrothermal treatment at 640 °C with 90% steam. Nijmeijer et al. [8] observed for pure γ -alumina, calcined at 825 °C, a pore growth from 4.2 to 6.2 nm after a hydrothermal treatment at 600 °C (100 h, $H_2O/CH_4 = 3/1$ (by volume) at 2.5 MPa total pressure). They showed that doping γ -alumina with 6% lanthanum could prevent this pore growth. Zahir et al. [9] also observed pore growth in undoped γ -alumina, calcined at 600 °C, after hydrothermal treatment at 500 °C. However, in their work it was found that, opposite to the findings of Nijmeijer et al., the addition of 6% lanthanum could not stop pore growth. Zahir et al. showed that only a mixture of 6% Lanthanum and 30% gallium in γ -alumina could prevent the pore growth during hydrothermal treatments. The reason for the difference between the results of

* Corresponding author.

E-mail address: m.w.j.luiten@utwente.nl (M.W.J. Luiten-Olieman).

Nijmeijer et al. and Zahir et al. might be the difference in calcination temperature used. The stabilization effects of lanthanum are due to the formation of lanthanumaluminate (LaAlO_3), which is only formed above 700 °C [10]. After calcination at 600 °C, as used by Zahir et al. [9], only lanthanum oxide is formed, which apparently does not contribute to the hydrothermal stability, while Nijmeijer et al. [8] used a calcination temperature of 825 °C.

Nagano et al. [11] doped nickel to γ -alumina to prevent pore growth in order to increase the hydrothermal stability. They found that the addition of 5% nickel was sufficient to prevent pore growth during hydrothermal treatments. Larger amounts of nickel led to the formation of nickel oxide and did not contribute to the hydrothermal stability of the membranes.

Nijmeijer et al. [8] have also shown that hydrothermal treatments of α -alumina supported γ -alumina membranes can lead to detachment of the γ -alumina layer from the support. They were successfully able to prevent this delamination by applying a monoaluminumphosphate (MAP) coating between the α -alumina support and the γ -alumina layer. The idea was that the chemical bonding between the support and γ -alumina by MAP is able to overcome the stresses induced by phase transformations and sintering of γ -alumina. Gishti et al. [12] showed that phosphorus doping stabilizes the γ -alumina phase to higher temperatures. Phosphorus doping is often achieved by impregnation [13,14] or addition in the gel-phase [14,15] in the form of phosphoric acid or ammonium phosphate. After calcination the phosphorus is present as a phosphate at the grain boundaries of the alumina, retarding phase transformations.

Although several investigations have been done on the hydrothermal stability of pure and doped γ -alumina intermediate layers, only few long-term stability tests have been performed with membrane separation layers coated on pure (non-modified) γ -alumina. For long-term pervaporation tests Casticum et al. used non-modified γ -alumina as an intermediate layer for their hybrid sol-gel derived separation layers, based on 1,2-bis(triethoxysilyl)ethane (BTESE) [16]. These membranes were used in butanol dehydration at 95 °C and performed well for over more than one year. Also cobalt-silica membranes, prepared by the group of Da Costa are coated on non-modified γ -alumina and subjected to hydrothermal treatments without significant degradation [17,18]. This raises the question whether or not the stability of the intermediate layer plays a big role in the stability of such silica-derived membranes.

Investigations on the hydrothermal stability of sol-gel derived membranes often focus on the separation layers, not on the interplay between the different layers. In this work a systematic investigation is performed to comprehend the impact of water or water vapor on the hydrothermal stability of the complete membrane. By using a straightforward hydrothermal treatment test, γ -alumina and MAP-modified γ -alumina membranes were tested. Hydrothermal stability was monitored by performing permeometry measurements on as-calcined membranes and hydrothermally treated membranes. The hydrothermal stability of the membranes coated with a BTESE separation layer was further evaluated by single gas permeation measurements on as-calcined as well as on hydrothermally treated membranes.

2. Experimental

2.1. Membrane preparation

As starting material for the γ -alumina layer a boehmite sol was used, prepared by the procedure as described elsewhere [2]. In short, aluminum-tri-sec-butoxide was precipitated in water of 90 °C and peptized by HNO_3 to obtain a boehmite sol with a par-

ticle size of around 50 nm. Prior to coating, the boehmite sol was mixed with a PVA solution, which acts as a binder and drying aid.

Disc shaped, porous α -alumina supports (pore size 80 nm, porosity 35%) with a diameter of 39 mm and a thickness of 2 mm (Pervatech B.V. the Netherlands) were coated under cleanroom conditions with a boehmite sol followed by a calcination at 650 °C (heating- and cooling rate of 1 °C/min, dwell time of 3 h.) This procedure was repeated once. Monoaluminumphosphate (MAP) modification was performed by coating the α -alumina supports with a 5 wt% MAP (Fluka) water solution. After MAP coating, the supports were calcined at 300 °C with a heating and cooling rate of 1 °C/min and a dwell time of 3 h prior to coating the boehmite sol.

BTESE sols were prepared by the following procedure: 1.04 mL of a 1.77 mol/L HNO_3 solution was added to 5.53 mL ethanol and placed in an ice bath. Subsequently 3.33 mL of BTESE (1,2-bis(triethoxysilyl)ethane) was added drop-wise to the mixture under vigorous stirring to obtain a final molar ratio of BTESE:EtOH: HNO_3 : H_2O of 1:10.8:0.2:6. The mixture was allowed to react at 60 °C for 90 min and put in an ice bath to quench the reaction. Ethanol was added to the solution to dilute the sol for dip coating to a final silicon concentration of 0.3 mol/L. Further details are given in [19]. This BTESE “dip sol” was coated once on the γ -alumina as well as on the MAP modified γ -alumina membranes under cleanroom conditions. The membranes were fired under nitrogen at 400 °C with a heating rate of 0.5 °C/min and a dwell time of 3 h.

2.2. Hydrothermal treatment

The hydrothermal treatment was performed in a reflux setup at ambient pressure. The membrane was placed in a holder with the separation layer facing upwards, and placed 2 cm above the water level in the reflux setup. The water was heated by an oil bath with a temperature of 110 °C to ensure a steam temperature of 100 °C, resulting in a relative humidity (RH) of 100% around the membrane. The test was continued for 72 h, after which the membrane was removed from the setup and dried in air at room temperature.

2.3. Characterization

Permporometry was performed in a home-made equipment to determine the pore size of the mesoporous layer. The pore-size of the membrane was determined using cyclohexane as the condensable gas, nitrogen as a carrier gas and oxygen for measuring the diffusional flux through the membrane as function of the vapor pressure of the condensable gas. The desorption mode was used to determine the actual pore-size of the membrane, using the Kelvin equation, which relates partial pressure of the condensable gas to a pore size. Full details about the equipment and the calculation method used can be found in the paper by Cao et al. [20].

High resolution scanning electron microscopy (SEM) was performed with a Zeiss Merlin FESEM on membrane cross-sections to study the thickness and morphology of the layers. The cross sections were placed on a sample holder and partly covered with aluminum tape to prevent sample charging. No further pretreatment was done on the samples and images were acquired at an accelerating voltage of 1 kV. For EDX the accelerating voltage was increased to 10 kV to make sure all the elements were detectable.

The membrane performance was characterized by means of single gas permeation. The membranes were measured in a “dead-end” mode. A feed pressure of 3 bara was applied to the membrane, while the permeate pressure was kept at atmospheric pressure. The pressure difference over the membrane was measured by a differential pressure sensor (GE Druck STX2100). The flow through the membrane was determined by a Bronkhorst EL-FLOW mass flow meter. The membranes were pretreated by heating to 200 °C under

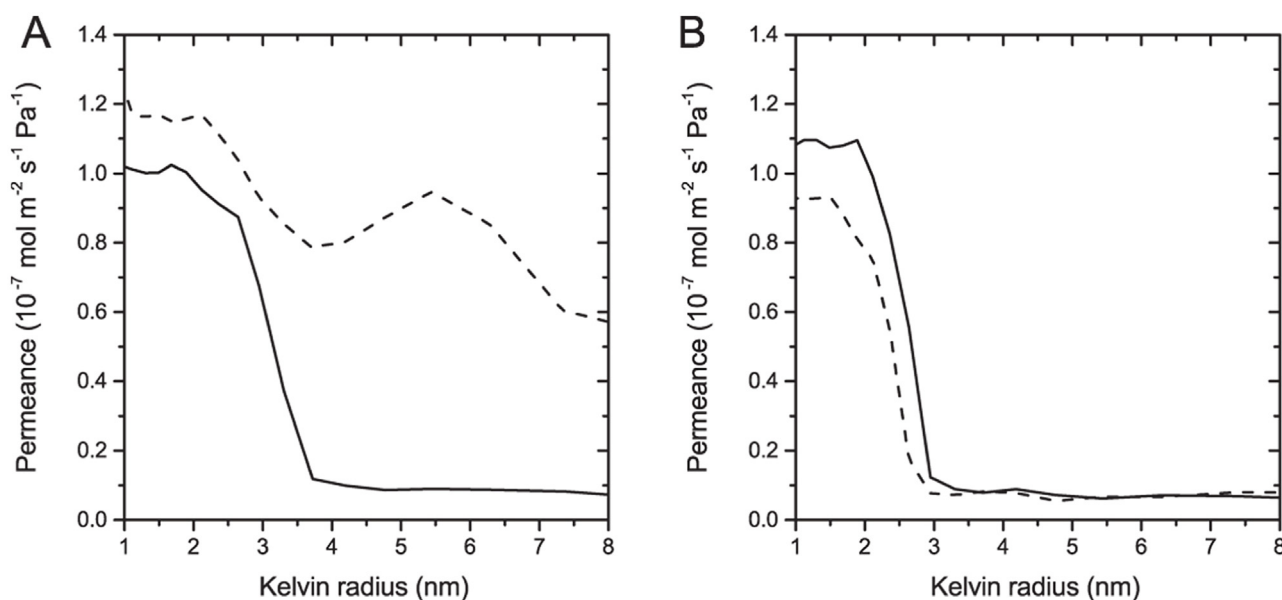


Fig. 1. Permporometry results of (A) γ -alumina and (B) MAP modified γ -alumina membrane layers as prepared (solid line) and after hydrothermal treatment (dashed line).

a helium flow with a rate of $1.5^\circ\text{C}/\text{min}$ to ensure complete removal of water from the membranes. After this conditioning step, the following gases were measured (in order of measurement): He, N_2 , CH_4 , H_2 , and CO_2 . Measurements were performed at 200°C with a transmembrane pressure of 2 bar. All gases were equilibrated for at least half an hour to ensure a constant flux. Two membranes were made from each sol and gas permeation results were averaged over the two membranes. The difference between the two membranes measured was within the experimental error.

3. Results and discussion

3.1. Hydrothermal stability of γ -alumina and MAP modified γ -alumina membranes

The average pore size of the γ -alumina and MAP modified γ -alumina membranes was determined by permporometry before and after the hydrothermal treatment. In Fig. 1 the results are depicted showing the oxygen permeance as function of the Kelvin radius. Based on these results the mean pore radius, before the hydrothermal treatment, could be calculated for γ -alumina and MAP modified γ -alumina membranes as being 2.7 and 2.0 nm resp. After the hydrothermal treatment the pore radius for the MAP modified γ -alumina membrane was reduced slightly from 2.0 to 1.7 nm. For the γ -alumina membrane no pore size could be determined by permporometry. In Fig. 1A no transition point is visible in permeance versus Kelvin radius for this membrane after the hydrothermal treatment, indicating that either the pores have grown to a pore radius of more than 20 nm (as being the upper limit of the used permporometry analysis method) or that large cracks or voids are formed.

The morphology of the membranes after the hydrothermal treatment was studied with SEM on membrane cross-sections. In Fig. 2 a SEM image of a hydrothermally treated MAP modified γ -alumina membrane is shown. No visible changes are observed after hydrothermal treatment.

In contrast to this, a large decay of the γ -alumina membrane is observed after the hydrothermal treatment. In Fig. 3 three SEM images are depicted of the γ -alumina membrane after the hydrothermal treatment. The SEM image of Fig. 3A gives a general overview of the surface in which two regions can be distinguished:

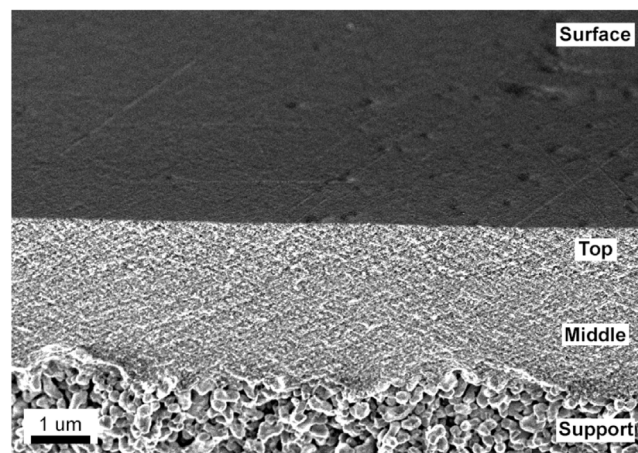


Fig. 2. SEM micrograph of hydrothermally treated MAP modified γ -alumina, the designations middle and top correspond to the first and second γ -alumina coating layer respectively.

a relative smooth surface with visible cracks and circle-shaped conglomerates with a diameter of about 1 μm , consisting of several particle-like structures. A detailed SEM image of the relative smooth surface is displayed in Fig. 3B showing some cracks, delamination of the layer and surface erosion. The layer thickness is varying between 2 and 2.5 μm , which is slightly thinner as compared to a not hydrothermally treated γ -alumina membrane (layer thickness of 3 μm). The observed cracks are in line with the observations made by Nijmeijer et al. [8] for a pure γ -alumina membrane after a hydrothermal treatment for 100 h at 600°C . In Fig. 3C a close-up of a circular conglomerate is depicted, consisting of “aggregates” with diameters varying from 5 to 50 μm . It seems that the aggregates are formed on the top of the γ -alumina membrane. The middle layer (also a γ -alumina layer) seems to be intact, suggesting some dissolution and recrystallization of membrane material.

In order to get a better understanding of the type of material in these aggregates EDX analysis was performed on the hydrothermally treated γ -alumina membrane, see Fig. 4. The letters in the image correspond to the data points, given in Table 1. The atomic ratios were calculated from the EDX results. The aggregates (data

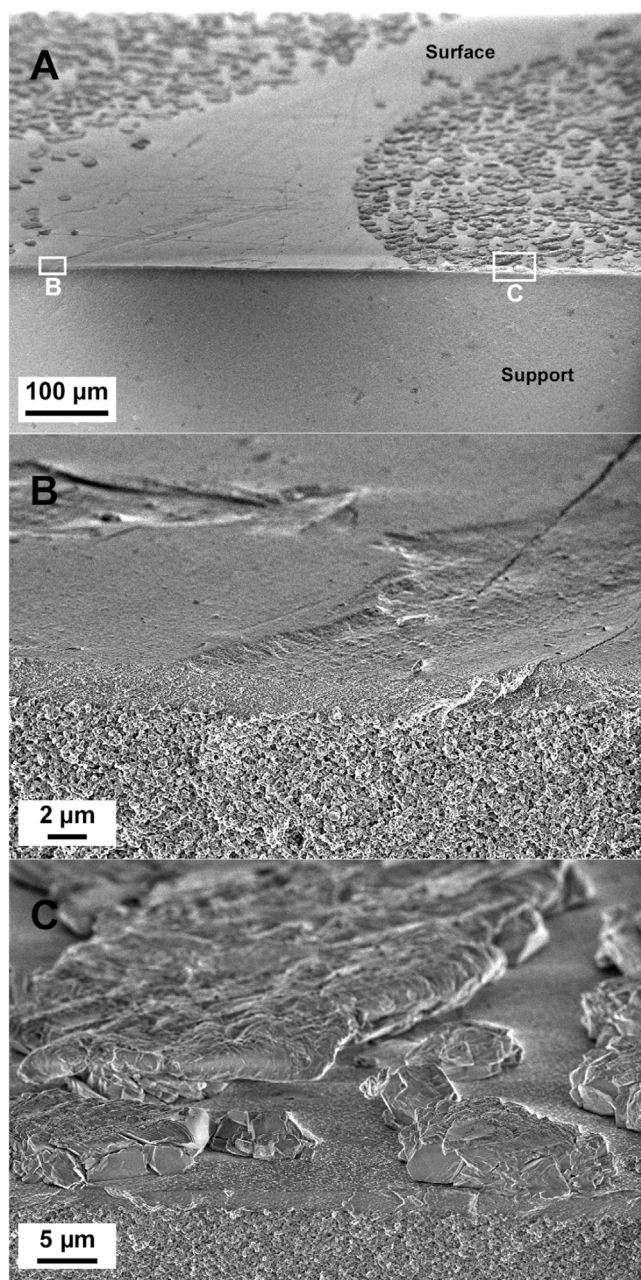


Fig. 3. SEM micrographs of hydrothermally treated γ -alumina. Overview of surface with circle shaped conglomerates (A), detail of surface between conglomerates (B), detail of surface in the conglomerate with aggregates in the range of 5–50 μm (C).

Table 1
EDX results from SEM image in Fig. 4.

Position	Al (atom%)	O (atom%)	Phase
A	28	72	$\text{AlOOH}/\text{Al}(\text{OH})_3$
B	29	71	$\text{AlOOH}/\text{Al}(\text{OH})_3$
C	39	61	Al_2O_3
D	45	55	Al_2O_3

points A and B in Fig. 4) have an Al:O atomic ratio of around 1:2.5, which corresponds to a 50:50 mixture of AlOOH and $\text{Al}(\text{OH})_3$. The thin, continuous layer (C) and the support (D) have an Al:O ratio of around 1:1.5 and corresponds to Al_2O_3 .

As mentioned before, the aggregates on the surface have an elemental composition that corresponds to a mixture of AlOOH and $\text{Al}(\text{OH})_3$. In literature [21–23] bayerite ($\text{Al}(\text{OH})_3$) and boehmite

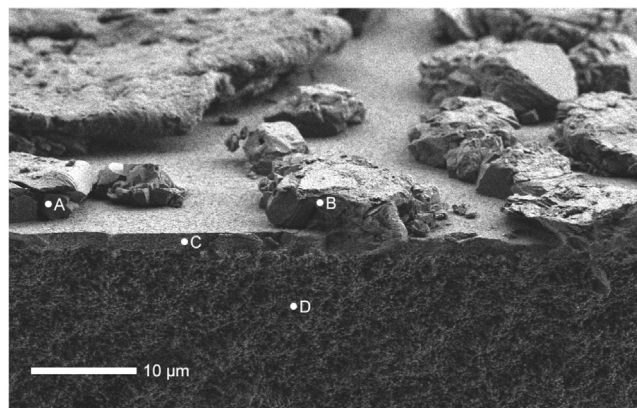


Fig. 4. SEM micrograph of hydrothermally treated γ -alumina containing “aggregates” on the surface. The letters correspond to the regions where an EDX measurement has been done.

Table 2
EDX results for MAP modified γ -alumina before and after hydrothermal treatment.

Atom ratio Al:P		
As-prepared	Top	1:0.03
	Middle	1:0.04
	Support	1:0.02
After treatment	Top	1:0.10
	Middle	1:0.11

(AlOOH) were observed in aqueous suspensions of γ -alumina, which were left for two months at room temperature. Lefèvre et al. [24] showed that γ -alumina is slowly hydrating in water at room temperature resulting in the formation of bayerite by first forming an intermediate amorphous phase. This bayerite phase was already found after immersion of γ -alumina for four days in water. The higher temperature of 100 °C, used in our work, probably accelerates these reactions resulting in the formation of boehmite and bayerite phases after 72 h of hydrothermal treatment. During the hydrothermal treatment water droplets were observed on the membrane surface and the circular shape of the regions with aggregates, observed in Fig. 3A, could be the result of the presence of these water droplets. Zahir et al. [9] also observed some small aggregates (1.8–5.3 μm) on the surface of γ -alumina after hydrothermal treatment, but no further investigations were done on the formation of this aggregates.

EDX analyses were also performed on as-prepared and hydrothermally-treated MAP-modified γ -alumina membranes as displayed in Fig. 2. The calculated atomic ratios are given in Table 2. The designations middle and top correspond to the first and second γ -alumina coating layer respectively (see experimental section). In the as prepared membranes small amounts of phosphorus were detected in the γ -alumina top layer as well as in the α -alumina support. After hydrothermal treatment a significant increase in phosphorus in the γ -alumina layer is observed.

During the calcination treatment at 650 °C after coating of the boehmite sol the phosphorus migrates through the alumina. This thermal migration is not a fast process, since the phosphorus content in the γ -alumina is very small before hydrothermal treatment (see Table 2, the as-prepared material). It seems however that the phosphorus migration is accelerated by water during hydrothermal testing as after this treatment about three times more phosphorous per unit of volume is present in the γ -alumina layer.

It is shown by Gishti et al. that phosphate ions strongly interacts with γ -alumina through a mechanism involving surface basic sites [12]. It is assumed that the strained Al–O–Al groups have the character of conjugated Lewis acid–base sites, forming surface

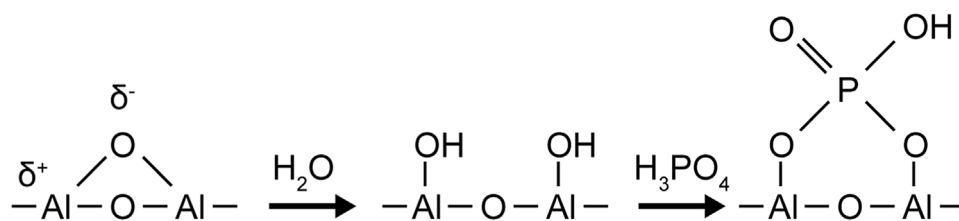


Fig. 5. Stabilization mechanism of phosphorus on alumina, as proposed by Gishti [12].

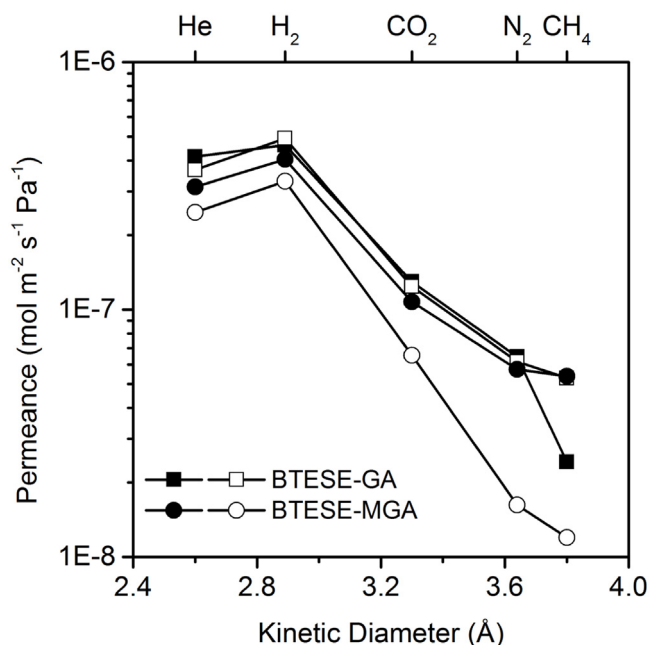


Fig. 6. Single gas permeation results of BTESE on a γ -alumina membrane (GA) and a MAP modified γ -alumina membrane (MGA). Closed symbols are as-prepared membranes; open symbols are hydrothermally treated membranes.

hydroxyl groups during reaction with water. The mechanism of this stabilization, as proposed by Gishti et al., is shown in Fig. 5. It is demonstrated by these authors that phosphate ions are irreversibly adsorbed on alumina, resulting in a modification/reduction of its surface reactivity and they claim that phosphate is unique in stabilizing strained Al-O-Al sites [12].

Zheng et al. [25], who studied the interaction of phosphate solution and mesoporous γ -alumina by in-situ ATR-FTIR spectroscopy, also describe this mechanism. They showed that 5 different phos-

phate alumina surface complexes were formed after flushing the mesoporous γ -alumina membranes with a phosphate solution ($\text{NaH}_2\text{PO}_4 \cdot \text{H}_2\text{O}$ and water) at different pH's. Moreover, it was observed that at pH 9.0 only 33% of a phosphate solution was adsorbed if compared with the amount adsorbed at pH 4. This was ascribed to the reduced fraction of AlOH_2^+ surface sites and the increased fraction of AlO^- sites upon increasing pH from 4 to 9.

As a result of this reaction of phosphate ions with the surface hydroxyl groups, the active sites for nucleation or adsorption [12,13,26], are deactivated resulting in an increased hydrothermal stability of the membrane.

3.2. BTESE layer on γ -alumina and MAP modified γ -alumina

In a second series of experiments a BTESE sol-gel layer was applied on the mesoporous γ -alumina and the MAP modified γ -alumina membrane. The Kelvin radius of these BTESE membranes could not be determined by permoporometry as these pores have a Kelvin radius below the detection limit of 1 nm [27–31]. Therefore single gas permeation measurements were performed to obtain an indication of the pore size. In Fig. 6 the gas permeances of several gases are depicted as function of the gas kinetic diameter. The BTESE on γ -alumina membranes showed a similar performance before and after hydrothermal treatment. These results are in agreement with our previous results on non-hydrothermally treated BTESE membranes [19]. Based on these results, it seems that, due to the coverage of the BTESE top layer, the γ -alumina layer remains intact during the hydrothermal treatment.

The single-gas permeance results, as depicted in Fig. 6, show a slightly lower permeance for all gases for BTESE coated on a MAP-modified γ -alumina membranes after hydrothermal treatment as compared to BTESE coated on γ -alumina membranes. Moreover, this decrease is more pronounced for the bigger gases like CO_2 , N_2 , and CH_4 resulting in an increase of almost a factor 3 in selectivity for H_2/N_2 (from 7 to 20). This phenomenon can be explained by looking at the permoporometry results of the MAP-modified γ -alumina membrane after hydrothermal treatment (see Fig. 1B).

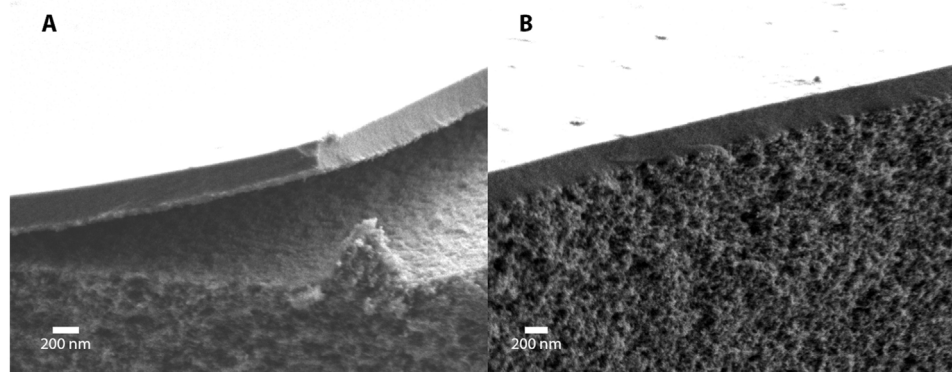


Fig. 7. SEM micrographs of hydrothermally treated BTESE on a γ -alumina membrane (A) and MAP modified γ -alumina membrane (B). The detachment in A has partially happened during imaging.

After hydrothermal treatment a slight shrinkage of the pores has occurred (mean radius decreases from 2.0 to 1.7 nm). It seems now that during the hydrothermal treatment of the BTESE-coated MAP-modified γ -alumina membrane the shrinking γ -alumina pores results in compressive forces in the BTESE layer and consequently a reduction in pore size of this BTESE separation layer.

SEM pictures were taken to investigate the membranes further. Fig. 7 shows SEM micrographs of BTESE coated on γ -alumina and MAP-modified γ -alumina membranes after hydrothermal treatment. In both cases the γ -alumina layer seems to have remained intact, which implies that the intermediate layer still has the original thickness of around 3 μm and no aggregates or cracks were formed. However, for the γ -alumina intermediate layer severe detachment of the BTESE layer is observed (see Fig. 7A). Initial detachment caused by sample treatment for SEM (meaning fracturing of the membrane) was visible by eye, but further detachment occurred during SEM imaging due to charging effects. Nijmeijer et al. [8] also observed delamination of the γ -alumina intermediate layer for a pure silica membrane after an hydrothermal treatment for 100 h at 600 °C.

The reason why a γ -alumina membrane coated with BTESE is not degrading in the way as is observed for a bare γ -alumina membrane, and why here a detachment of the BTESE layer occurs, will now be discussed. Due to the hydrophobic coating the γ -alumina surface is not accessible for liquid water, but only for water vapor. Therefore no dissolution and recrystallization can take place, which otherwise will form the type of aggregates as observed for bare γ -alumina after this hydrothermal treatment (see Fig. 4). However, a phase transformation of γ -alumina to boehmite or bayerite, which was shown for a bare γ -alumina membrane, can occur resulting in a volume increase. The stresses at the interface between γ -alumina and BTESE, caused by this phase transformation severely weakens the adhesion between these layers, resulting in the delamination of the BTESE layer as observed in Fig. 7a. Fracturing, however, of the BTESE layer is prevented due to its flexibility.

A BTESE coating on a MAP modified γ -alumina membrane did not show any signs of delamination after hydrothermal testing. So, it can be concluded that the addition of MAP improved the attachment of the γ -alumina intermediate layer resulting in a more hydrothermal stable BTESE derived silica membrane. Although, during the thermal treatment still migration of the phosphorus occurs from the MAP intermediate layer to the upper γ -alumina layer. A straightforward pretreatment, of this MAP-modified γ -alumina membrane system at high water vapor pressure and 100 °C, could be applied allowing the migration to occur under controlled circumstances.

4. Conclusion

It is shown that a hydrothermal treatment at low temperature (100 °C) and high water activity strongly degrades a γ -alumina membrane. These results are in line with what is found in literature for tests at higher temperature and water vapor pressures.

Applying a coating of mono-aluminum phosphate (MAP) between α -alumina support and γ -alumina layer led to a hydrothermal stable γ -alumina membrane due to stabilization by phosphorus components. A BTESE coating on a MAP modified γ -alumina membrane did not show any signs of delamination after hydrothermal testing while severe detachment of the BTESE layer from the γ -alumina membrane was found during SEM imaging.

A pretreatment of this MAP-modified γ -alumina membrane system at high water vapor pressure and 100 °C results in a hydrothermally stable membrane due to an accelerated migration of phosphorus into the γ -alumina layer. The phosphate anions strongly interact with γ -alumina resulting in a deactivation of the

strained Al-O-Al groups which have the character of conjugated Lewis acid-base sites. As result of this deactivation the surface hydroxyl groups, the active sites for nucleation or adsorption, are neutralized resulting in a hydrothermally-stable γ -alumina layer. Therefore MAP modification can be a viable way of stabilizing γ -alumina.

Moreover, a factor 3 increase in H_2/N_2 (perm)selectivity was observed in gas permeation experiments of a hydrothermally treated MAP modified γ -alumina membranes, coated with a hybrid silica (BTESE-derived) separation layer. So besides the improvement in thermal stability also an increase in selectivity is realized.

Acknowledgments

We acknowledge financial support for this research from ADEM, A green Deal in Energy Materials of the Ministry of Economic Affairs of The Netherlands (www.adem-innovationlab.nl). Furthermore we would like to acknowledge Dion Smink for his assistance with the experimental work.

References

- [1] L.M. Gandia, G. Arzamendi, P.M. Dieguez, Renewable Hydrogen Technologies Production, Purification, Storage Applications and Safety, Elsevier B.V., 2013.
- [2] R.J.R. Uhlhorn, et al., Synthesis of ceramic membranes, *J. Mater. Sci.* 27 (2) (1992) 527–537.
- [3] A.F.M. Leenaars, A.J. Burggraaf, The preparation and characterization of alumina membranes with ultrafine pores. 2. The formation of supported membranes, *J. Colloid Interface Sci.* 105 (1) (1985) 27–40.
- [4] T. van Gestel, et al., Potentialities of microporous membranes for H_2/CO_2 separation in future fossil fuel power plants: evaluation of SiO_2 , ZrO_2 , Y_2O_3 - ZrO_2 and TiO_2 - ZrO_2 sol-gel membranes, *J. Membr. Sci.* 359 (1–2) (2010) 64–79.
- [5] S. Araki, et al., Preparation and pervaporation properties of silica-zirconia membranes, *Desalination* 266 (1–3) (2011) 46–50.
- [6] E.E.E. Dorre, Aluminum oxide, a wear resistant, high-temperature material for manifold applications, *Veitsch-Radex Rundsch.* 1–2 (1983) 128–132.
- [7] G.R. Gallaher, P.K.T. Liu, Characterization of ceramic membranes I. Thermal and hydrothermal stabilities of commercial 40 Å membranes, *J. Membr. Sci.* 92 (1) (1994) 29–44.
- [8] A. Nijmeijer, et al., Preparation and properties of hydrothermally stable γ -alumina membranes, *J. Am. Ceram. Soc.* 84 (1) (2001) 136–140.
- [9] M.H. Zahir, et al., Preparation and properties of hydrothermally stable γ -alumina-based composite mesoporous membranes, *J. Am. Ceram. Soc.* 89 (9) (2006) 2874–2880.
- [10] A.K. Adak, P. Pramanik, Synthesis and characterization of lanthanum aluminate powder at relatively low temperature, *Mater. Lett.* 30 (4) (1997) 269–273.
- [11] T. Nagano, et al., Hydrothermal stability of mesoporous Ni-doped γ -alumina, *J. Ceram. Soc. Jpn.* 117 (1367) (2009) 832–835.
- [12] K. Gisht, et al., On the role of phosphate anion in the MoO_3 - Al_2O_3 based catalysts, *Appl. Catal.* 12 (4) (1984) 381–393.
- [13] R.L. Cordero, et al., Surface changes of alumina induced by phosphoric acid impregnation, *Appl. Catal.* 56 (1) (1989) 197–206.
- [14] J. Wang, et al., Effect of phosphorus introduction strategy on the surface texture and structure of modified alumina, *Microporous Mesoporous Mater.* 121 (1–3) (2009) 208–218.
- [15] W. Gu, et al., Gelification process to prepare phosphate modified alumina: study on structure and surface properties, *J. Alloys Compd.* 441 (1–2) (2007) 311–316.
- [16] H.L. Castricum, et al., High-performance hybrid pervaporation membranes with superior hydrothermal and acid stability, *J. Membr. Sci.* 324 (1–2) (2008) 111–118.
- [17] S. Battersby, et al., Hydrothermal stability of cobalt silica membranes in a water gas shift membrane reactor, *Sep. Purif. Technol.* 66 (2) (2009) 299–305.
- [18] D. Uhlmann, S. Smart, J.C. Diniz da Costa, High temperature steam investigation of cobalt oxide silica membranes for gas separation, *Sep. Purif. Technol.* 76 (2) (2010) 171–178.
- [19] H.F. Qureshi, A. Nijmeijer, L. Winnubst, Influence of sol-gel process parameters on the micro-structure and performance of hybrid silica membranes, *J. Membr. Sci.* 446 (2013) 19–25.
- [20] G.Z. Cao, et al., Permporometry study on the size distribution of active pores in porous ceramic membranes, *J. Membr. Sci.* 83 (2) (1993) 221–235.
- [21] C. Dyer, et al., Applications of fourier transform Raman spectroscopy/3-llsurface hydration of aqueous γ - Al_2O_3 studied by Fourier transform Raman and infrared spectroscopy—I. Initial results, *Spectrochim. Acta Part A: Mol. Spectrosc.* 49 (5) (1993) 691–705.

- [22] E. Laiti, P. Persson, L.-O. Öhman, Balance between surface complexation and surface phase transformation at the alumina/water interface, *Langmuir* 14 (4) (1998) 825–831.
- [23] H. Wijnja, C.P. Schulthess, ATR–FTIR and DRIFT spectroscopy of carbonate species at the aged γ -Al₂O₃/water interface, *Spectrochim. Acta Part A: Mol. Biomol. Spectrosc.* 55 (4) (1999) 861–872.
- [24] G. Lefèvre, et al., Hydration of γ -alumina in water and its effects on surface reactivity, *Langmuir* 18 (20) (2002) 7530–7537.
- [25] T.-T. Zheng, et al., Sorption of phosphate onto mesoporous γ -alumina studied with in-situ ATR–FTIR spectroscopy, *Chem. Cent. J.* (2012) 6.
- [26] G.A.H. Mekhemer, et al., Surface to bulk characterization of phosphate modified aluminas, *Colloids Surf. A: Physicochem. Eng. Aspects* 161 (3) (2000) 439–446.
- [27] M. ten Hove, A. Nijmeijer, L. Winnubst, Facile synthesis of zirconia doped hybrid organic inorganic silica membranes, *Sep. Purif. Technol.* 147 (2015) 372–378.
- [28] M. Kanezashi, et al., Organic–inorganic hybrid silica membranes with controlled silica network size: preparation and gas permeation characteristics, *J. Membr. Sci.* 348 (1–2) (2010) 310–318.
- [29] J.E. Ten Elshof, A.P. Dral, Structure–property tuning in hydrothermally stable sol–gel processed hybrid organosilica molecular sieving membranes, *J. Sol-Gel Sci. Technol.* 79 (2016) 279–294.
- [30] H.L. Castricum, et al., Tuning the nanopore structure and separation behavior of hybrid organosilica membranes, *Microporous Mesoporous Mater.* 185 (2014) 224–234.
- [31] G. Li, M. Kanezashi, T. Tsuru, Preparation of organic–inorganic hybrid silica membranes using organoalkoxysilanes: the effect of pendant groups, *J. Membr. Sci.* 379 (1–2) (2011) 287–295.